Industrial Engineering Journal
ISSN: 0970-2555
Volume : 53, Issue 8, August : 2024

Design and Simulation of Bidirectional DC-DC Converter Topology for Battery Applications

[1]J. Manoj [2]V. Hemalatha
[1]Research Scholar, Dept of EEE, Chirala Engineering college, Chirala, Bapatla Dist.., AP
[2]Assist. Professor, Dept of EEE, Chirala Engineering college, Chirala, Bapatla Dist.., AP

Abstract.
Different factors affect solar photovoltaic (PV) systems by decreasing input energy and reducing the conversion efficiency of the system. One of these factors is the effect of snow cover on PV panels, a subject lacking sufficient academic research. This paper reviews and compares current research for snow removal in solar PV modules. Additionally, this paper presents the design, analysis and modelling of a smart heating system for solar PV Electric Vehicle (EV) charging applications. The system is based on a bidirectional DC-DC converter that redirects the grid/EV-battery power into heating of the solar PV modules, thus removing snow cover, as well as providing the function of MPPT when required to charge the EV battery pack. A control scheme for each mode of operation was designed. Subsequently, a performance evaluation by simulating the system under various conditions is presented validating the usefulness of the proposed converter to be used in solar PV systems under extreme winter conditions.

1 Introduction

Different studies have revealed the potential of various renewable energy sources to be utilized for human energy consumption in the world; among all the energies, solar energy is the most promising due to its high potential (3,850,000 EJ) [1]. Despite its huge potential, the production of solar energy to contribute to the power supply demand is not significant [1,2]. At the same time, there are different limitations in solar PV systems that have made their implementation slow since their appearance. Some of the limitations of solar PV systems include price (the relation between lifetimes generation cost versus electricity prices), energy storage, and efficiency, among others. According to Ueda et al. [3] the efficiency of solar PV systems can be affected by meteorological parameters that decrease the input energy such as shading, soiling, snow covering, mismatch, etc.; or parameters that reduce the conversion efficiency such as module temperature, losses, equipment efficiency, and others [3].

Most of these factors have been researched in-depth, such as the effects of shading and mismatch or the efficiency of the converters used, resulting in an improvement in system efficiency [4–10]. The current converters developed have an efficiency of around 90% or higher; however, more research is still required to improve the input energy efficiency of solar PV cells [11–14]. Many studies have been developed on the effects of snowfall on solar PV systems since this is one of the main factors affecting the performance of PV systems in cold areas [10,15–32].

Several active and passive heating systems for snow removal of PV modules have been proposed in the literature. In Canada, the company Soltek Solar Energy Ltd. (Victoria, BC, Canada) developed flush mount panels to reduce the snow covering issue on solar across the surface. There have also been attempts to create acephobic surface coatings, which repel ice or inhibit ice formation [20,27,30,32,33]. However, there are no conclusive and effective results related to these materials. Ross and

Usher [33,34] proposed a heating system that melts snow using reflected radiation from the ground to heat the back surface of the PV module by using a black absorbent coating placed on the back of the module mounted alongside with a glass enclosure, although the results found were negligible.

In the existing literature, research presented in [9] reports the design and analysis of BDC based solar photovoltaic (PV) system. The bidirectional buck-boost operation is shown with open loop control using simulation results.

In [10], a detailed loss analysis and theoretical model to determine the efficiency of the BDC are studied. Also, converter's efficiency is analysed in terms of the effect of temperature, switching frequency and duty ratio. Experimental findings are given to demonstrate the feasibility of the developed model.

A logic control scheme is developed for BDC based BESS in [11]. The small signal model for buck and boost operation is presented to control the BDC via averaging and linearization technique. Simulation tests are performed to show the performance of the designed control scheme.

Reference [12] suggests a time delay control as a solution to address the nonlinear characteristics of BDC based lithium-ion battery application. To show the superior performance of the designed controller, it is compared with proportional-integral (PI) control and the experimental implementation is carried out for verification.

Research reported in [13] presents the design and modelling of a solar PV electrical vehicle based on BDC. A control method is introduced by giving simulation results under various atmospheric conditions.

In this paper, a non-isolated BDC with a buck and boost operating concept is designed and simulated through a number of case studies. Within the designed system, the BDC controls the bidirectional power flow between battery and DC-link. During the charging stage of a battery working in buck mode, the battery is fed from the DC-link, and the battery current is regulated by the BDC through the use of PI controller. Conversely, in the discharge stage of the battery operating in boost mode, when the DC source is disconnected, the battery supplies power to the DC load. The BDC ensures the control of the DC-link voltage using PI controller during this process. The operation and control of the BDC is shown by the simulation results under various scenarios.

Including this introductory section, the overall structure of the study consists of four sections. Section 2 explains the circuit structure, operation and control of BDC with battery application. Simulation study of BDC is reported in Section 3. Lastly, the conclusions are presented in Section 4.

2 BDC topology and battery application

The circuit configuration of the non-isolated BDC topology is represented in Figure 1. There are several advantages of this topology such as allowing the bidirectional energy transfer, compact size and high efficiency [14, 15]. As given in Figure 1, BDC has two switching elements (S_1 and S_2), two diodes (D_1 and D_2), two capacitors (C_1 and C_2) and one inductor (L). MOSFET or IGBT can be used as a switching element in the circuit implementation of this topology. Basically, in order to transfer the energy in two directions, BDC can operate in buck and boost mode.

The following section provides detailed descriptions of the component design of the proposed bidirectional buck-boost converter that guarantees operation in any mode of operation. However, before going into details, the following assumptions will be considered during the analysis:

• All the components are considered ideal; ON period forward voltage drops and equivalent series resistance (ESR) of the components are neglected.

• The selection of the inductor (L1) is such that the converter always operates in continuous conduction mode (CCM);

• The output voltage ripple is negligible.

• In steady state operation, both the integral of Volts-sec through an inductor, as well as the integral of Amp-sec through a capacitor, during one cycle will be equal to zero. Figure 1 depicts the framework of the bidirectional buck-boost DC-DC converter proposed for the snow removal and charging application.

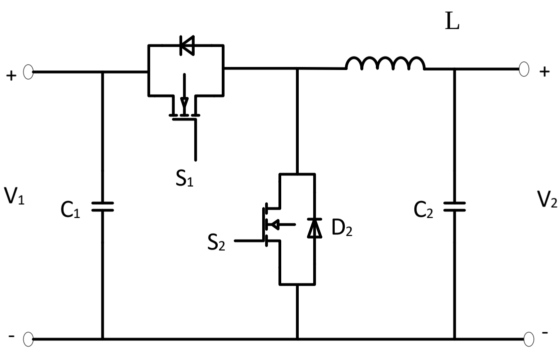

Fig. 1. Circuit structure of the BDC topology.

2.1 Buck mode operation

In this mode, BDC operates in the forward operating mode. The energy from the V1 source is transferred to the V2 side. The connection between input voltage (V1) and output voltage (V2) is explained as follows:

$$k_{D1} = \frac{V_2}{V_1} \quad (1)$$

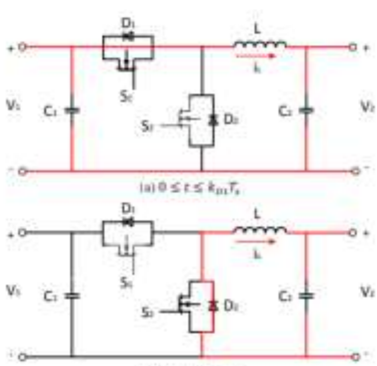

Fig. 2. Buck mode operation cases.

2.2 Boost mode operation

In this mode, BDC operates in the backward operation mode. The energy stored in the inductor and V_2 power source such as battery supplies to the DC load in the V_1 part. The relation between input voltage (V_2) and output voltage (V_1) is expressed as

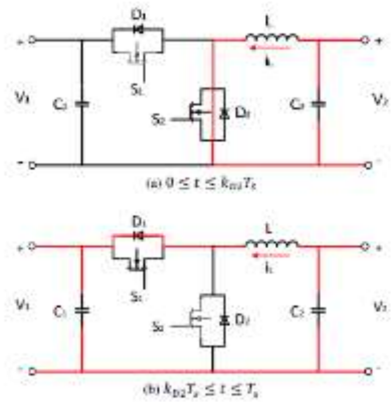

Fig. 3. Boost mode operation cases.

The schematic diagram of power system including BDC and battery is demonstrated in Figure 4. While any renewable energy source such as wind and solar power can be used as voltage source, simple DC power source is also employed. DC load is fed from the DC-link whose energy is supplied from voltage source or battery. In this configuration, BDC controls the battery current in a bidirectional manner. In buck mode operation, while battery is charging, load is fed from the voltage source. On the other hand, in boost mode operation, during the disconnection of voltage source, while battery is discharging, load is fed from the battery.

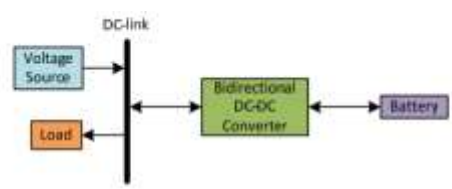

Fig. 4. Overall schematic diagram of BDC with battery system

Figure 5 shows the control block diagram of buck mode operation. Voltage source is enabled on DC-link side and battery is charging by regulating the battery current using PI controller. In addition, control scheme for boost

Industrial Engineering Journal
ISSN: 0970-2555
Volume : 53, Issue 8, August : 2024

mode operation is presented in Figure 6. Accordingly, when the voltage source is disabled or unavailable due to the external conditions, DC-link and load is fully fed from the battery.

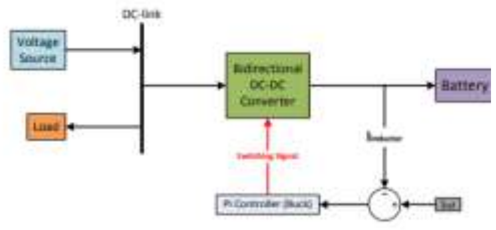

Fig. 5. Control loop for buck (charging) mode

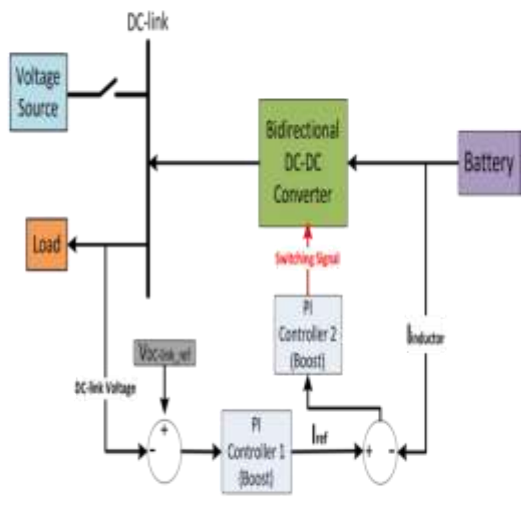

Fig. 6. Control loop for boost (discharging) mode.

Table 1. Design parameters.

Parameter	Value	Parameter	Value
Voltage source (V_1)	120 V	Battery type	Lithium-ion
Battery voltage	48 V	Battery capacity	100 Ah
Switching frequency	15 kHz	Battery initial SOC	50
DC-link capacitance	10 mF	Load resistance	10 •
Inductor (L)	10 mH	Load inductance	5 mH

Table 2. Controller parameters

Control Unit	Value
PI controller (Buck)	Kp=0.004 Ki=9.5
PI controller 1 (Boost)	Kp=0.02 Ki=6
PI controller 2 (Boost)	Kp=0.002 Ki=0.6

3 Simulation study

BDC based BESS is designed and simulated under various scenarios in this work. Circuit parameters of the designed model are given in Table 1. Controller parameters of the designed system are given in Table 2. All simulations are conducted under RL load condition, which is connected to DC-link side of the BDC.

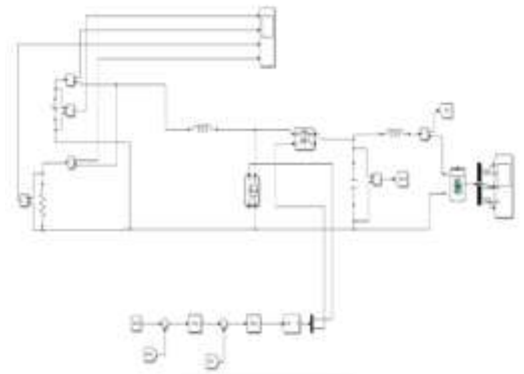

3.1 Buck mode operation

3.1.1 Case Study 1: Constant reference current

In this case, the power is transferred from DC-link to the battery. Accordingly, the simulation is conducted with constant reference current mode. Control loop given in Figure 5 is activated by setting the reference current to 20

Industrial Engineering Journal
ISSN: 0970-2555
Volume : 53, Issue 8, August : 2024

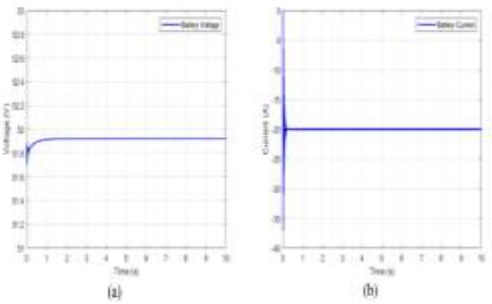

(b)

Fig. 7. (a) Battery voltage, (b) battery current on case 1 for buck mode

A. Figure 7(a) and 7(b) show the battery voltage (approximately 51.9 V) and battery current (-20 A), respectively. From those values, the power absorbed by the battery is nearly equal to 1038 W. According to the Figure 8, the BDC inductor current follows the reference set current as 20 A. Battery stateof-charge (SOC) is increasing at a constant rate meaning that the battery is charging, as given in Figure 9.

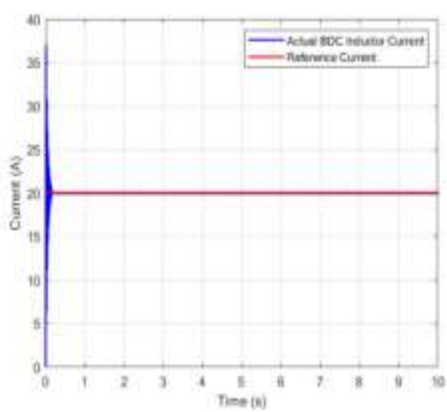

Fig. 8. BDC inductor current and reference

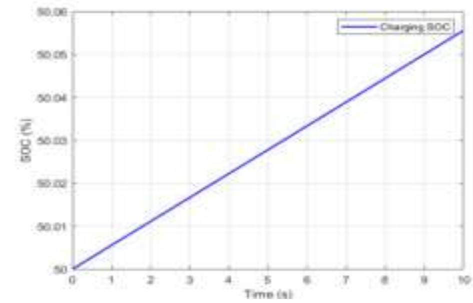

Fig. 9. Battery SOC on case 1 for buck mode. current on case 1 for buck mode.

3.1.2 Case Study 2: Variable reference current

In this scenario, the power is also transferred from DC-link to the battery. The simulation is done with variable reference current mode. Control scheme presented in Figure 5 is activated by setting the reference current to 20 A, 40 A, 10 A and 30 A, respectively. The controller reference current change is determined by selecting 4 s time intervals. Figure 10(a) and 10(b) demonstrate the battery voltage and battery current, respectively. While battery voltage is around 52 V, battery current is regulated at -20 A, -40 A, -10 A and -30 A, respectively. From those values, the power absorbed by the battery is nearly equal to 1038 W, 2086 W, 518 W and 1563 W, respectively. According to the Figure 11, the BDC inductor current follows the reference set current during the whole simulation. Battery SOC is increasing at different rates meaning that the battery is charging, as given in Figure 12.

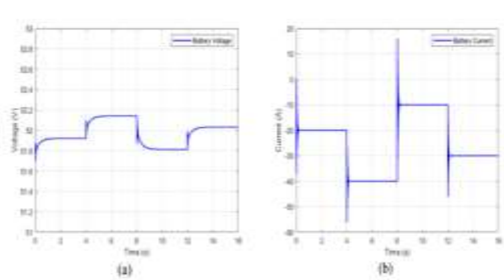

(b)

Fig. 10. Battery voltage (a), battery current (b) on case 2 for buck mode.

Industrial Engineering Journal
ISSN: 0970-2555
Volume : 53, Issue 8, August : 2024

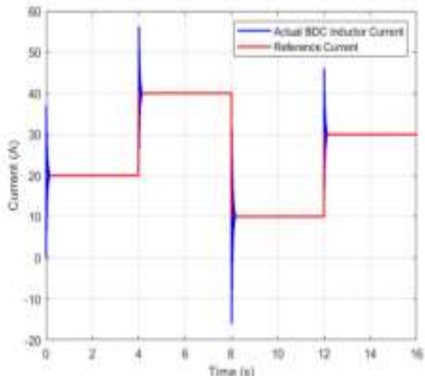

Fig. 11. BDC inductor current and reference

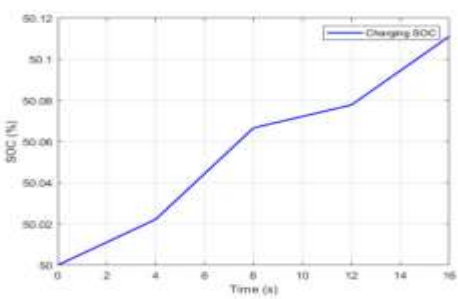

Fig. 12. Battery SOC on case 2 for buck mode. current on case 2 for buck mode.

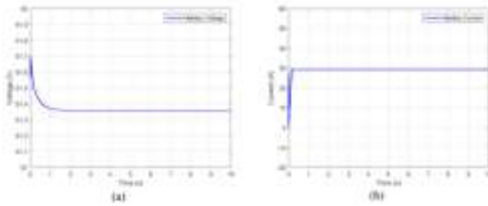

(b)

Fig. 13. Battery voltage (a), battery current (b) on case 1 for boost mode.

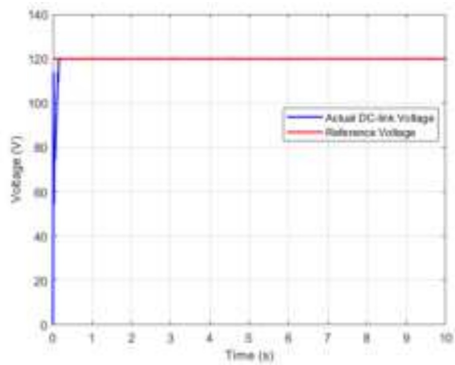

Fig. 14. DC-link voltage and reference voltage

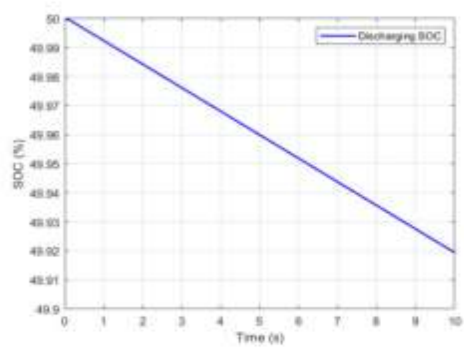

Fig. 15. Battery SOC on case 1 for boost mode. on case 1 for boost mode.

3.2 Boost mode operation

3.2.1 Case Study 1: Constant DC-link voltage

The power is transferred from battery to the load in this case analysis. The simulation is carried out with constant DC-link voltage mode. Control scheme depicted in Figure 6 is activated by setting the reference DC-link voltage to 120 V. Figure 13(a) and 13(b) show the battery voltage (approximately 51,36 V) and battery current (29 A), respectively. From those values, the power delivered by the battery is nearly equal to 1489 W.According to the Figure 14, DC-link voltage follows the reference voltage as 120 V. Battery SOC is decreasing at a constant rate meaning that the battery is discharging, as given in Figure 15.

3.2.2 Case Study 2: Variable DC-link voltage

The power is also transferred from battery to the load in this case analysis. The simulation is conducted with variable DC-link voltage mode. Control scheme presented in Figure 6 is activated by setting the reference DC-link voltage to 120 V, 140 V, 100 V and 130 V, respectively. The controller reference voltage change is specified by selecting 4 s time intervals. Figure 16(a) and 16(b) show the battery voltage and battery current, respectively. While battery voltage is around 51.3 V, battery current is nearly regulated at 30 A, 40 A, 20 A and 35 A, respectively. From those values, the power delivered by the battery is nearly equal to 1539 W, 2052 W, 1026 W and 1795 W, respectively.

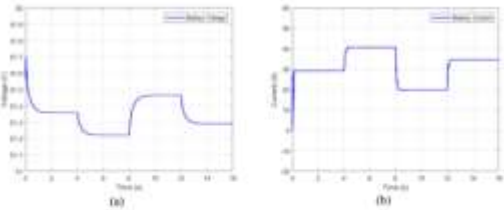

(b)

Fig. 16. Battery voltage (a), battery current (b) on case 2 for boost mode.

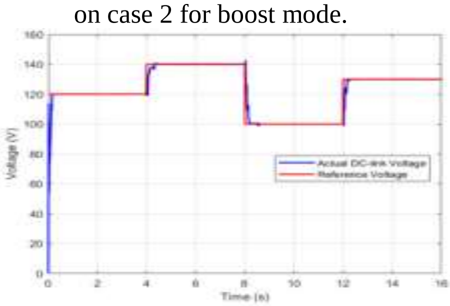

Fig. 17. DC-link voltage and reference voltage

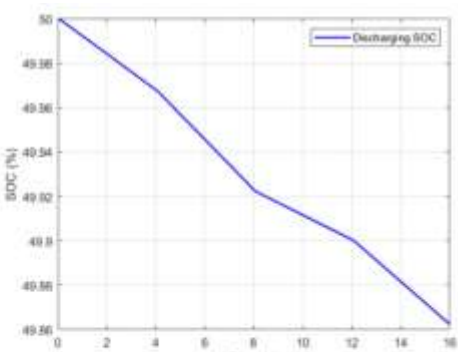

Fig. 18. Battery SOC on case 2 for boost mode. on case 2 for boost mode.

According to the Figure 17, DC-link voltage follows the reference voltage during the whole simulation.Battery SOC is decreasing at different rates meaning that the battery is discharging, as given in Figure 18.

4 Conclusion

Over the past few decades, energy storage has gained importance for power electronics applications based on renewable energy sources. Batteries are an attractive choice for energy storage and they are widely adopted by renewable energy sources, electrical vehicles and grid connected systems. In battery applications, bidirectional power flow control by regulating the charging and discharging stage of battery is achieved by BDC. Accordingly, the battery current is controlled by adjusting the duty cycle of the BDC by taking into account the state of charge of the battery and current direction. In this work, a non-isolated BDC, has a buck and boost principle of operation, has been designed, analyzed and simulated under various scenarios. In the simulated system, BDC controls the bidirectional power flow between battery and DC link. In this context, in buck mode, battery has been fed from the DC-link and the battery current has been controlled via PI controller. On the other hand, in boost mode, when DC source is disconnected, DC load has been fed from the battery and DC-link voltage is regulated by BDC using PI controller. The simulation results have been presented to demonstrate the operation and control of the BDC under different case studies.

References

1. A. A. Kebede, T. Kalogiannis, J. Van Mierlo, M. Berecibar, A comprehensive review of stationary energy storage devices for large scale renewable energy sources grid integration, Renew. Sustain. Energy Rev., **159**, p. 112213, (2022)
2. Y. Sun, Z. Zhao, M. Yang, D. Jia, W. Pei, B. Xu, Overview of energy storage in renewable energy power fluctuation mitigation, CSEE J. Power Energy Syst., **6** (1), pp. 160–173, (2020)
3. S. Hajiaghasi, A. Salemnia, M. Hamzeh, Hybrid energy storage system for microgrids

applications: A review, J. Energy Storage, **21**, pp. 543–570, (2019)

4. A. G. Olabi, C. Onumaegbu, T. Wilberforce, M. Ramadan, M. A. Abdelkareem, A. H. Al – Alami, Critical review of energy storage systems, Energy, **214**, p. 118987, (2021)
5. M. M. Rahman, A. O. Oni, E. Gemechu, A. Kumar, Assessment of energy storage technologies: A review, Energy Convers. Manag., **223**, no. May, p. 113295, (2020)
6. N. Padmanabhan, M. Ahmed, and K. Bhattacharya, Battery Energy Storage Systems in Energy and Reserve Markets, IEEE Trans. Power Syst., **35** (1), pp. 215–226, (2020)
7. R. Rajasekaran & P. U. Rani, Bidirectional DC-DC Converter for Microgrid in Energy Management System, Int. J. Electron., **108** (2), pp. 1–22, (2020)
8. T. Sutikno, R. A. Aprilianto, and H. S. Purnama, Application of non-isolated bidirectional DC–DC converters for renewable and sustainable energy systems: a review, Clean Energy, **7** (2), pp. 293–311, (2023)